

Modeling of the Chiroptical Response of Chiral Amino Acids in Solution Using Explicit Solvation and Molecular Dynamics

Matthew D. Kundrat and Jochen Autschbach*

Department of Chemistry, 312 Natural Sciences Complex, The State University of New York at Buffalo, Buffalo, New York 14260-3000

Received December 1, 2008

Abstract: Molecular dynamics (MD) simulations and TDDFT linear response computations were employed to model the molar rotations of the zwitterionic forms of glycine, alanine, proline, and phenylalanine in aqueous solution. The MD simulations inherently take into account averaging the chiroptical response of different amino acid conformers and also allow the effects from vibrational distortions and explicit solvent perturbations on the optical rotation to be modeled. The results show that the chiroptical response correlates strongly to the conformations of these molecules relative to their carboxylate functional groups. Additionally, the molar rotation of phenylalanine shows a correspondence to the molecule's internal rotation about its phenyl group. These findings may be rationalized with established and revised "sector rules" for optical activity.

Introduction

Molar rotation is among the quintessential properties of chiral molecules. A solution of one enantiomer of a chiral compound will rotate the polarization plane of polarized light either to the left or the right, depending on the absolute configuration of the molecule. Matching the computed molar rotation of such a chiral molecule with experiment to assign its absolute configuration has drawn significant interest, due in part to the advances in time dependent density functional theory (TDDFT), which allows for efficient routine calculations of optical rotations from first principles.^{1–10}

Most of the *ab initio* wave function based and density functional theory modeling of chirality done to date has been with static models of structurally rigid molecules. However, most chiral molecules found in nature can adopt multiple conformations, and are not frozen but are actively vibrating as they are measured at room temperature. Modeling the chiroptical response of flexible molecules by time dependent density functional theory computations on static conformers and averaging their responses based upon respective Boltzmann factors has met with some success.^{2,11–19} However, in addition to approximations intrinsic to TDDFT the overall

accuracy of such modeling is limited by the accuracy of the Boltzmann factors, which can be difficult to gauge.

Our most recent work in this area involved calculations on the small amino acids, glycine and alanine.²⁰ The publication served as a validation of the method of using force-field based (classical) molecular dynamics (MD) and an explicit point charge solvent model along with TDDFT to model the chiroptical response properties of these molecules. This MD-based modeling method has several purposes: First the molecular dynamics simulation serves as an engine to generate configurations of the molecules of interest in differing conformations, conformational sampling being essential to the modeling of chiroptical properties of flexible molecules. The second advantage of employing molecular dynamics is that it allows us, through capturing many geometries from the simulation, to model some of the thermal effects on chirality, for instance from vibrations; these effects have drawn much attention from our research group and others.^{8,21–30} Third, the molecular dynamics simulation contains explicit water molecules, which through the simple point charge model can serve as an effective means of modeling solvation effects, whose import impact on optical rotation has drawn significant interest as well.^{10,11,25,28,30–40}

In keeping with prior publications on the chiroptical response of amino acids,^{20,41} this work begins with calcula-

* Corresponding author phone: (716) 645-6800 x2086; fax: (716) 645-6963; e-mail: jochena@buffalo.edu.

tions on glycine, the smallest amino acid. In a recent work, glycine was used to benchmark a method of explicit solvation using point charge water molecules and molecular dynamics to model chiroptical response. Here the method is used to explore the variations in this response with respect to changes in the geometry of the glycine molecule. While not intrinsically chiral, glycine can through the course of molecular dynamics adopt chiral configurations which give rise to nonzero molar rotations. In fact, those molar rotations can be very large. The first section investigates the regular variations of this chiral response as a function of glycine's N–C–C–O dihedral angle over the course of a molecular dynamics simulation and how differing solvation models affect this molar rotation. Comparable trends in the chiroptical response of the smallest chiral amino acid, alanine, are also discussed. The regular variations of molar rotation are correlated with sector rules for amino acid chiroptical activity.

The focus of the paper then shifts to proline, a chiral amino acid known to adopt two different conformations at room temperature, differing in the direction of puckering for its five membered ring. The relative populations of these two conformers obtained by classical molecular dynamics are found to be remarkably similar to that obtained by DFT and those derived from experiment. The dependency of molar rotation upon this configuration is found to be similar to that seen for fixed configurations optimized with DFT. The variation of molar rotation with the N–C–C–O dihedral angle is similar to that of glycine, but with the variations expected from the fact that proline is intrinsically chiral and glycine is not.

The next section deals with phenylalanine, a more conformationally flexible chiral amino acid which can be found in rotamers whose molar rotation depends on not one but two chromophores. As such, the effects of the rotamer identity, as well as dihedral angles, with respect to the carboxylate and phenyl chromophores, are examined. As with proline and glycine, the variation of the dihedral angle with respect to the COO[−] group (the N–C–C–O angle) causes variations in the molar rotation consistent with the sector rule for the carboxylate chromophore. The variation of the C_α–C_β–C_γ–C_δ dihedral angle, which relates directly to the geometry about the phenyl chromophore, yields results consistent with recent incarnations of the sector rule for the phenyl chromophore, which are the opposite of what the older sector rule for this group predicted.

Finally, the average molar rotations resulting from thousands of TDDFT calculations of proline and phenylalanine are compared with experiment. The populations of the three different phenylalanine conformers obtained from classical molecular dynamics are more evenly distributed than those obtained from the Boltzmann weighting of DFT optimized structures. The populations of the proline molecule computed by molecular dynamics and those obtained from Boltzmann weighted DFT optimizations both agree very well with experimentally derived values in the literature. This allows us to isolate the effects that the intrinsic dynamics of the solute and dynamic solvation have on the molar rotation for

this molecule in solution and to evaluate how well these factors are modeled by the current computational methods.

Computational Methods

Many of the computational methods used in this work are detailed in previous publications^{20,41–43} where TDDFT based computations of optical rotations of amino acids were exhaustively benchmarked. All quantum mechanical (QM) data were computed with the Turbomole⁴⁴ quantum chemical software, version 5.7.1. Dunning's aug-cc-pVDZ basis set⁴⁵ was used for all calculations except those involving the aromatic sector rule, which will be discussed later in this work. The PBE0 functional was employed, since for small amino acids in solution it yields low lying electronic excitations that are reasonably close to those obtained at the CC2 level of theory. For some calculations the conductor-like screening model (COSMO)⁴⁶ of solvation was applied to the ground state. Molar rotations were calculated at the wavelength of the sodium D line (589.3 nm) and reported in units of deg·cm²/(dmol). The center of the mass of the amino acid molecule has been used for the coordinate origin for all response calculations. While the molar rotations computed herein are attributed to the length representation of the electric dipole operator and are formally origin dependent, this dependence is minimized in TDDFT when large basis sets such as aug-cc-pVDZ are used; see our earlier work and the references cited therein.⁴¹

Geometries used in the quantum mechanical calculations were generated with the GROMACS⁴⁷ molecular dynamics program, version 3.3.3, in a fashion similar to that of Mukhopadhyay et al.³³ Molecular dynamics of solvated amino acid molecules were run in a cubic periodic solvent box measuring 25 × 25 × 25 nm³ with average density of 1.0 g/cc using TIP3P water molecules. Note that the phrases, "TIP3P solvation" and "COSMO solvation" will be used later in this article referring to subsequent DFT calculations which treat the solvent molecules as simple point charges taken from the TIP3P model and those which discard all the explicit water molecules from the molecular dynamics simulation and treat the solvent as a continuum. 256 water molecules from each MD configuration were used in any subsequent DFT calculations; as such, no water molecules greater than 12.5 nm from the center of the solute were included, yielding solvation spheres for QM calculations that were nearly spherical, not cubic. The all-atom OPLS-AA molecular mechanics (MM)⁴⁸ force field was used for the simulations, which were carried out at 300K with a time step of 1 fs. Snapshots of the simulations, akin to frames of a motion picture, were taken every 10 ps for glycine and 100 ps for the larger molecules, which was a sufficient duration for energetic and chiroptical response calculations of adjacent MD configurations to be uncorrelated. These geometric configurations were used for subsequent computations of molar rotation. The classical mechanics MD used here captures some of the dynamical effects on the optical rotation. Ideally, of course, the nuclear motion should be treated quantum mechanically. Zero-point and temperature-dependent vibrational and internal rotation corrections on optical rotation using approximate nuclear wave functions suitable for local minima have been considered by

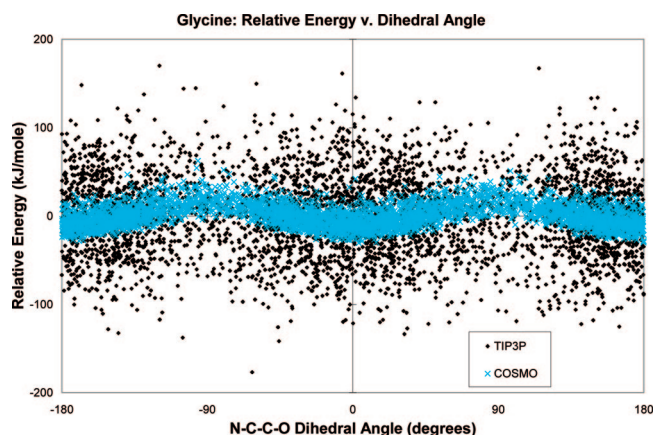


Figure 1. Variation of the energy of a glycine system as a function of the N–C–C–O dihedral angle. The energies reported include either 256 point charge based water molecules or the COSMO solvation model. All energies are reported relative to the average energy for the model. The geometries were generated by molecular dynamics with the GROMACS program, and snapshots were recorded at 10 ps intervals.

our group previously,^{21–24} but this approach has not been adapted for use with solvation models needed for this work. In many aspects the approximations used here and in those previous works are complementary and capture different aspects of the dynamical behavior of the system.

Results and Discussion

Effects of the Dihedral Angles on Energy and Molar Rotation for Glycine and Alanine. All the chiral amino acids studied here can be regarded as derivatives of glycine, the smallest amino acid. The functional groups in glycine and the structural variations thereof are present in the other amino acids as well, and so it is logical to investigate this prototypical molecule first. Among all the structural variables in glycine, one stands out as having the greatest impact on optical activity. It is the O–C–C–N dihedral angle, a structural portion which is present in all amino acids. As this angle varies during the course of a molecular dynamics simulation, the energy of the system and its chiroptical response vary as well. This section shows how the energy and molar rotation of glycine correlate strongly with this dihedral angle.

The relative energy of a solvated glycine molecule as a function of this angle is plotted in Figure 1. The reference point for this relative energy is the average energy at the PBE0/aug-cc-pVDZ level of theory using either explicit TIP3P waters or the COSMO solvent continuum; a comparison of the raw energies of the two different methods would not yield relevant results. The first detail of note from this graph is that the energy of the system varies much more when explicit point charge water molecules are used for solvation than when the COSMO continuum is used. This is to be expected since the large variations in the geometries formed by the explicit waters can lead to greater changes, both positive and negative, of the glycine–water system. For each DFT calculation with COSMO, the continuum is built

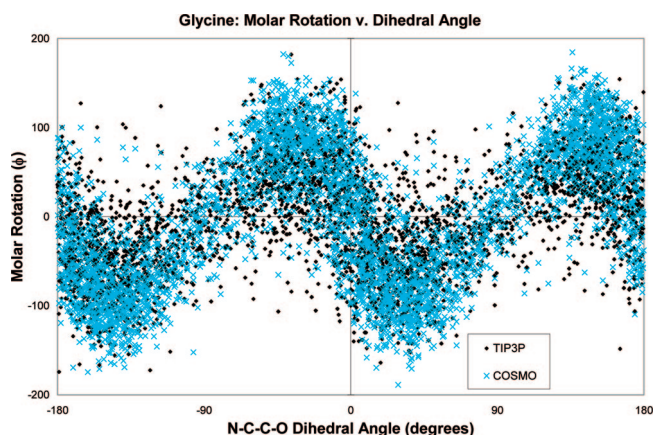


Figure 2. Molar rotation (ϕ) of glycine as a function of the N–C–C–O dihedral angle. The geometries used are from the same dynamics run used for Figures 1 and 5, and include either 256 point charge based water molecules or the COSMO solvation model.

around the glycine molecule, however distorted its geometry may be. For the calculations using explicit TIP3P waters, the positions and geometries of the solvent molecules can differ vastly between different snapshots of the MD, and how optimally a particular solvent sphere geometry may stabilize the solute varies considerably.

The second point we want to draw attention to in Figure 1 is the correlation between energy and clustering of structures. The energy of the system is calculated at the PBE0/aug-cc-pVDZ level of theory. The geometries with their particular dihedral angles are determined by the all-atoms force field in GROMACS. Depending on the details of the force field and solvent–solute interactions, the geometries of glycine that constitute local minima could potentially differ between the QM and MM methods, but they do not. The trend of the QM energies indicates that the molecule has a local minimum structure with its dihedral angle at 0° (or 180°, due to the degeneracy in the C_{2v} symmetrical carboxylate group). This is in agreement with the QM optimization calculations on glycine in our previous work.⁴¹ In that work we found the glycine structure with the $\pm 90^\circ$ dihedral to be a saddle point, which is consistent with the data in Figure 1. These data also indicate that the energetics of the MM simulation agree with the QM results.

While the energy of a solvated glycine molecule is an *even* function of its N–C–C–O dihedral angle, the molar rotation, depicted in Figure 2, is an *odd* function. The energy of the glycine molecule increases as the dihedral angle deviates from its ideal at 0°, regardless of the direction of the perturbation. The molar rotation, however, deviates in equal and opposite directions depending on which way the molecule twists. This is in keeping with the sector rule for optical rotation of amino acids.⁴³ As the N–C–C–O dihedral changes, the functional groups that perturb the symmetry of the otherwise C_{2v} symmetrical carboxylate group move either above or below the horizontal symmetry plane of that group. As the sign of the optical activity “sectors” are opposites on opposite sides of this plane, the molar rotation changes in opposing ways depending on which side of the plane those perturbing groups deviate from.

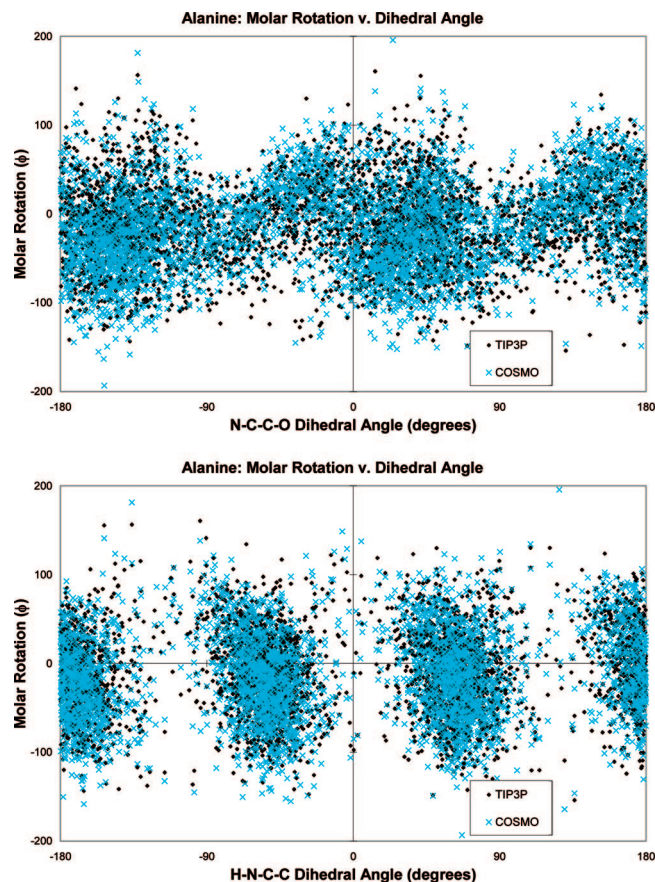


Figure 3. Molar rotation of a solvated alanine zwitterion as a function of the N–C–C–O (top) and H–N–C–C (bottom) dihedral angles.

Also note that every time that the N–C–C–O dihedral angle is an integer multiple of 90° , the molecule assumes approximate C_{2v} symmetry, but the optical rotation may be nonzero because of distortions elsewhere in the molecule as well as movement in the explicit solvation shell where one is present. It is useful here to draw attention to the works of Wiberg et al.,⁴⁹ in which the effects of torsional angles on optical activity were also demonstrated, and that of Pecul et al.,⁵⁰ where among other things the optical rotation of alanine was modeled. For a comparison with the latter we have performed MD simulations for the alanine zwitterion; the results of which are shown in Figure 3. The plots both show periodic variations of optical rotation as a function of the N–C–C–O dihedral angle. A notable difference is that our plot for the zwitterionic glycine, as well as our results from calculations with the zwitterionic form of alanine depicted in Figure 3, with its C_{2v} symmetrical chromophore, shows symmetrical results when the chromophore is rotated 180° , while the plot for the neutral alanine,⁵⁰ with its COOH chromophore whose C_{2v} symmetry is significantly perturbed by its hydrogen atom, shows results that are not quite symmetrical about a 180° rotation.

Since, unlike glycine, alanine is a chiral molecule, the molar rotation need not average to zero when the N–C–C–O dihedral angle approaches a multiple of 90° , though since the molar rotation of alanine is known from experiment to be small (about $2 \text{ deg}\cdot\text{cm}^2/(\text{dmol})$) this deviation should not be too great. The variation of the molar rotation of alanine

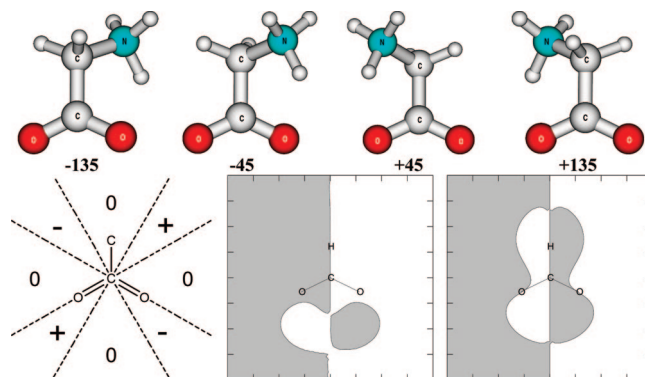


Figure 4. Glycine molecule with differing O–C–C–N dihedrals, Jorgensen's sectors for amino acids (depicted as a set of overlapping carbonyl chromophores, *not* a pentavalent carbon), and sectors computed from TDDFT for the CD of the first excitation (center) and molar rotation (right) of the formate anion (areas of positive rotation are light, negative areas are dark). Jorgensen's sectors shown are above the plane of the page, those below the plane are of the opposite sign. Note that the configurations of glycine with dihedral angles of $+45^\circ$ and -135° , as well as those of -45° and $+135^\circ$, are equivalent due to the symmetry of the carboxylate group.

with respect to the H–N–C–C dihedral angle, which describes the rotation of the NH_3^+ group, is shown on the bottom of Figure 3. The C_{3v} symmetry of this functional group is readily apparent from the periodicity of the graph, as is the fact that during the molecular dynamics simulation the NH_3^+ group shows a strong tendency to be found near its rotational minima at intervals 120° apart. The periodic variation of molar rotation for the NH_3^+ group is not as obvious, as it is dwarfed by the variation in molar rotation caused by the rotation of the COO^- group which is occurring simultaneously in the molecular dynamics simulation. This is consistent with the fact that for a zwitterionic alanine molecule the COO^- group is the primary chromophore effecting molar rotation at 589.3 nm , and the NH_3^+ group is secondary, just as it has been computed that for a neutral alanine in the gas phase the COOH group is the primary chromophore and the NH_2 group has secondary effects.⁵⁰

Returning to the less complex glycine molecule, the dihedral angles in Figure 2 that are multiples of 90° represent “nodes” in oscillating molar rotation pattern. These are the geometries in which the glycine molecule is most symmetrical, and as such its molar rotations are the smallest in magnitude. Conversely, when the N–C–C–O dihedral angle deviates most from multiples of 90° , the molar rotations tend to be the greatest. Some configurations of glycine where this configuration is far from symmetrical are depicted in Figure 4.

According to a sector rule model for amino acid optical activity derived from CD sector rules by Jorgensen,⁵¹ the glycine configurations with the NH_3^+ group in a positive sector should have positive molar rotation, and those with the NH_3^+ group in a negative sector should have a negative molar rotation. Our computations of a formate anion (to model the carboxylate chromophore), perturbed with a negative point charge, form sectors which are consistent with

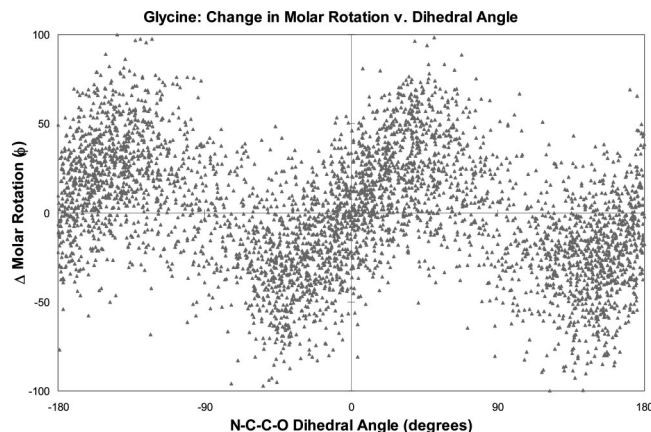


Figure 5. Difference between the molar rotation computed using point charge water molecules and that computed using the COSMO solvent model. $\Delta\phi = \phi_{\text{TIP3P}} - \phi_{\text{COSMO}}$.

this as well. However, we point out that the sector modeling of glycine by formate is a rather crude model; see our previous publication for details⁴³ and note the differing signs of the computed CD and optical rotation sectors close to around the C–H bond. The data in Figure 2 confirm that the sector assignment yields the expected sign of the optical rotation. For the conformers where the dihedral angle is near $+45^\circ$ (or -135° , due to the degeneracy caused by the symmetrical COO^- group), the molar rotation is negative. For those molecules with O–C–C–N dihedrals nearing -45° (or $+135^\circ$), the molar rotation is positive.

One interesting factor that deserves attention is the effect of explicit solvation as a function of dihedral angle on molar rotation. This effect is implied in Figure 2, which shows the molar rotation of glycine solvated by explicit point charge water molecules and that solvated by a continuum. However, the differences are not obvious in Figure 2; therefore, the difference of these two molar rotations has been computed explicitly, and the results are shown in Figure 5.

The periodic “wave” pattern formed by the data in Figure 5 appears to be a somewhat weakened mirror image of the data in Figure 2, as the maxima in Figure 2 coincide with the minima in Figure 5 and vice versa. The rationale for this pattern correlates with the sector rule, and the fact that the location of a perturbing group relative to the carboxylate chromophore affects the optical rotation of the glycine molecule. Here the perturbing entities causing the change in the chiroptical response are not the glycine’s NH_3^+ group but the water molecules surrounding it. Due to the nature of the molecular dynamics simulation of a liquid system where the molecules are in close contact, the water molecules occupy the space not taken by the glycine solute. So if the NH_3^+ group happens to occupy a *negative* sector, then the ensemble of water molecules surrounding it will preferentially occupy the *positive* sectors. As such, the use of explicit point charge waters to solvate glycine as opposed to a continuum model has a damping effect on the resulting optical activity.

Proline. The chiral amino acid proline shares the same carboxylate chromophore as its achiral counterpart, glycine. Therefore, one would expect the N–C–C–O dihedral angle

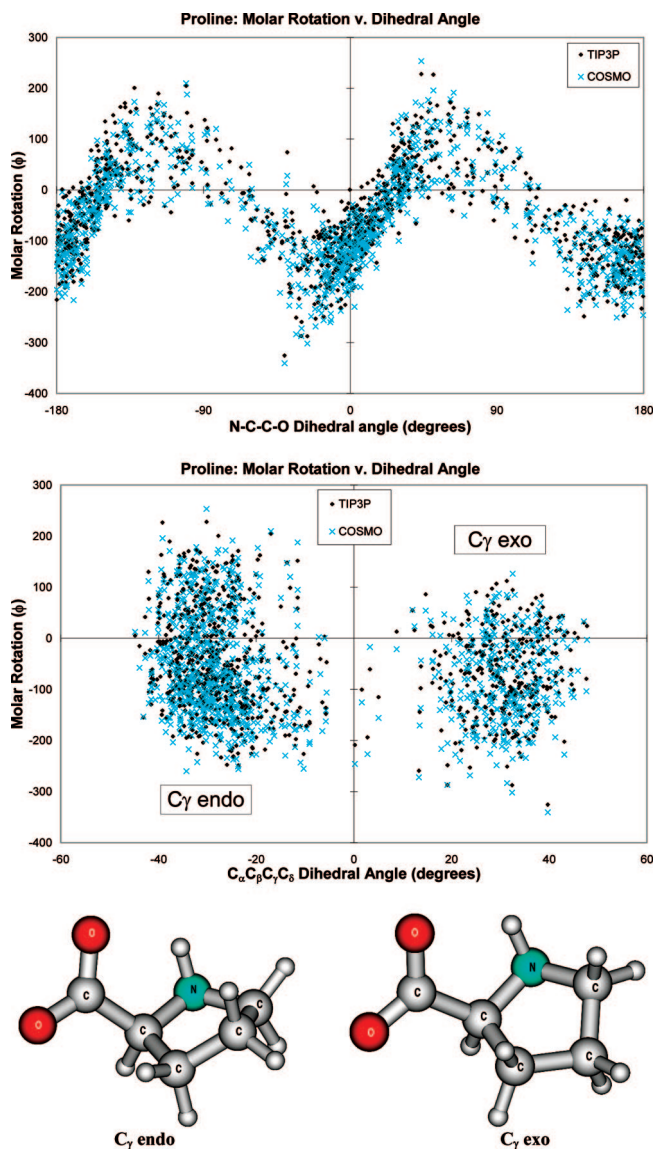


Figure 6. Molar rotation of proline as a function of its N–C–C–O (upper plot) and $\text{C}_\alpha\text{--C}_\beta\text{--C}_\gamma\text{--C}_\delta$ (lower plot) dihedral angles, along with illustrations of the proline molecule in its C_γ endo (left structure) and C_γ exo (right structure) conformations. The $\text{C}_\alpha\text{--C}_\beta\text{--C}_\gamma\text{--C}_\delta$ dihedral angle is indicative of the envelope conformation of the five-membered ring. If this angle is negative, the molecule is in the C_γ endo conformation; if it is positive, it is C_γ exo.

for this molecule to have a profound effect on its molar rotation as well. As can be seen in Figure 6, this is indeed the case.

The upper plot of Figure 6 has some similarities to the corresponding graph for the glycine molecule. (Note that only 1024 configurations were sampled here compared to 4096 for glycine, since the relative size of the proline molecule required more TDDFT computing time per configuration.) As with glycine, the optimal dihedral angle is close to 0° , which again is in agreement with the geometries optimized by first principles methods. The data also repeat after a period of 180° , owing to the C_{2v} symmetry the carboxylate group possesses in both molecules. Differences can be seen where this periodic wave intercepts zero. In glycine, the molar rotation approaches zero when this dihedral angle approaches

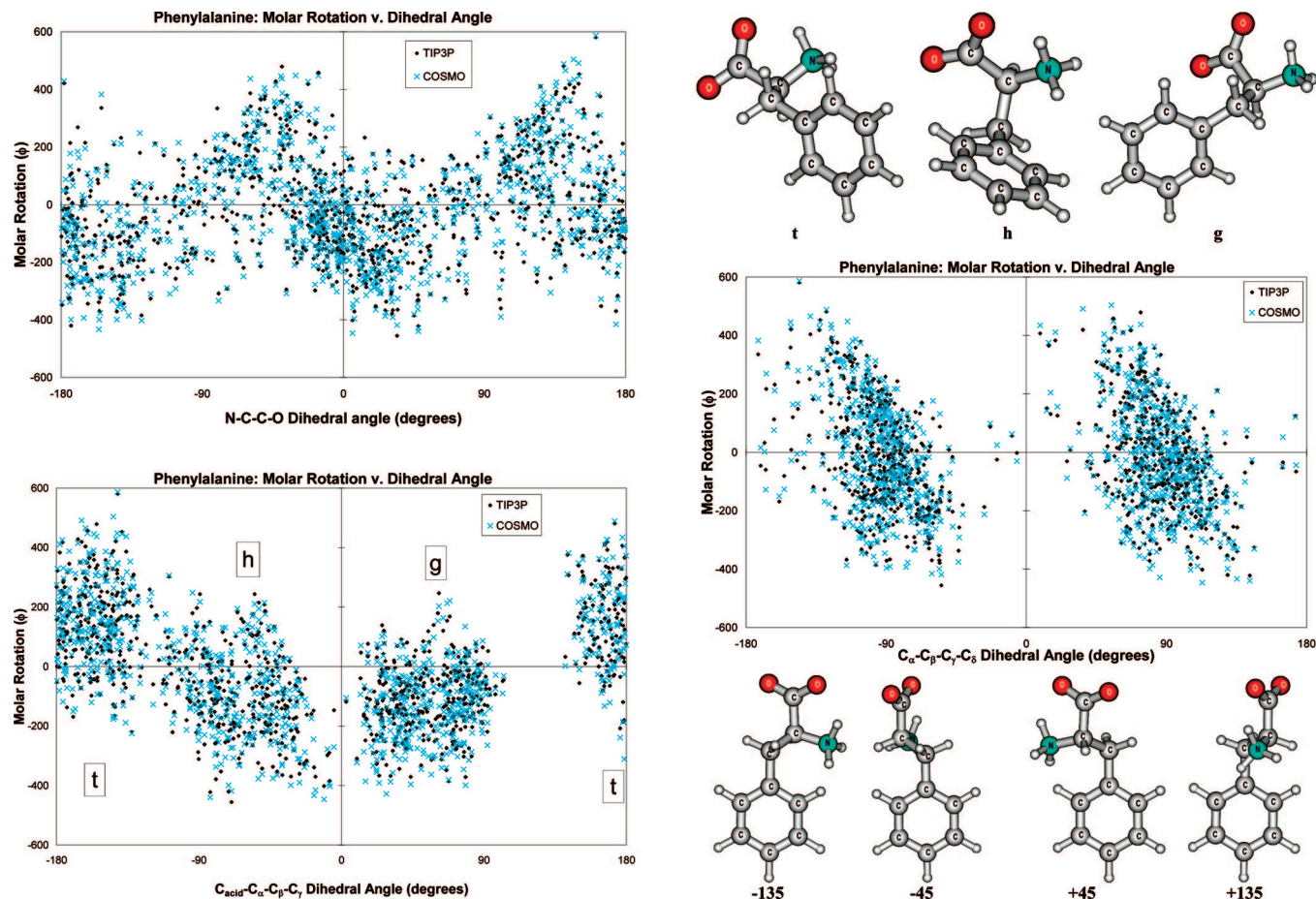


Figure 7. Molar rotation of phenylalanine as a function of its N-C-C-O (top left plot), C_{acid}-C_α-C_β-C_γ (bottom left plot), and C_α-C_β-C_γ-C_δ (right plot) dihedral angles, along with illustrations of phenylalanine in relevant conformations. The C_{acid}-C_α-C_β-C_γ dihedral defines the molecule as being in a trans (t), gauche (g), or hindered (h) conformation. The C_α-C_β-C_γ-C_δ dihedral angle is indicative of how the aromatic ring is twisted with respect to the rest of the molecule.

zero. In proline, this is not the case. Proline, unlike glycine, is inherently chiral in its various conformers. From static DFT calculations⁴¹ and from experimental data, we expect this rotation to be negative. Indeed, the MD average yields about $-100 \text{ deg}\cdot\text{cm}^2/(\text{dmol})$.

It is known both from experiment and prior calculations that the proline molecule tends to form two optimal structures, both significantly populated at room temperature and differing only by the puckering of the ring; see our earlier work and the references cited therein.⁴¹ Prior DFT calculations and some experiments concur that the conformation with the γ carbon in the endo configuration is slightly favored. This more populous conformation has been previously shown to have a molar rotation that is somewhat less negative than its less populous C_γ exo counterpart. The bottom portion of Figure 6 confirms that both the energetic and molar rotation trends seen with frozen isolated proline configurations are reproduced by the molecular dynamics based calculations in this work. In this instance, the C_γ endo conformations, those having a negative C_α-C_β-C_γ-C_δ dihedral angle, have a relative “population” of 66% and an average molar rotation of -41.0 with TIP3P waters and -53.9 with COSMO, while the C_γ exo conformers form the balance of the population and have an average molar rotation of $-68.1 \text{ deg}\cdot\text{cm}^2/(\text{dmol})$ with TIP3P waters and $-81.6 \text{ deg}\cdot\text{cm}^2/(\text{dmol})$ with COSMO.

Phenylalanine. The amino acids investigated thus far show a periodic variation of molar rotation as a function of the molecule’s N-C-C-O dihedral angle. Phenylalanine, an aromatic amino acid, is no exception in this regard, as can be seen in the top of Figure 7. As phenylalanine has an average molar rotation that is closer to zero than does proline, the “phase” of the wave in its molar rotation plot is more similar to glycine. However, there is significantly more scatter in the molar rotations for phenylalanine than for glycine, or proline for that matter. This is due to a few factors. First, as result of its size and flexibility, phenylalanine has a larger conformational space than glycine or proline. It can be found in three rotamers, differentiated by their C_{acid}-C_α-C_β-C_γ dihedral angles, which have been shown to differ significantly in their individual specific rotations.⁴² Its phenyl functional group is free to flex and bend, moving into different sectors about the carboxylate chromophore even as the N-C-C-O dihedral remains the same, thus causing more variation in molar rotation for a given N-C-C-O dihedral value.

Another factor that may contribute to the scatter seen in the top of Figure 7 is that the phenyl functional group is itself a chromophore that can contribute to the calculated molar rotation. In a prior molecular modeling work⁴² this chromophore did not show a significant impact on molar

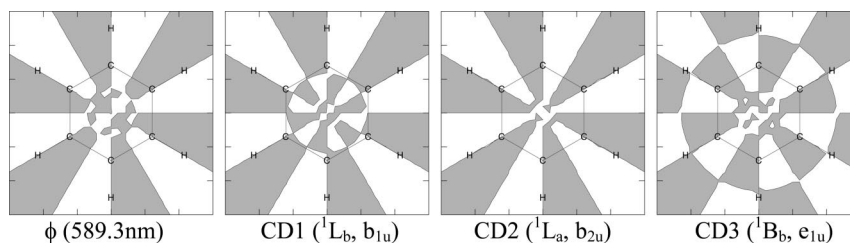


Figure 8. Sign of the molar rotation and CD of the first 3 electronic transitions of benzene as a function of the position of a perturbing group. Positive rotations are indicated by the light areas, while negative rotations are depicted by the dark areas. A point charge of -0.1 was used as a perturber, and the sectors drawn are 1.3 \AA above the plane of the ring. A grid size of 0.1 \AA was used, and the distortions along the edges of the contour lines (particularly evident in the center of the ring) are caused by the coarseness of the grid. The molar rotation calculations were performed at the PBE0/SVP level of theory, and the CD calculations with CC2/SVP.

rotation, since when held rigid the external perturbations did not perturb the chromophore enough to cause a significant contribution from the electronically forbidden π to π^* transition. But in this study which uses molecular dynamics to generate the geometries, the phenyl ring is free to vibrate, and such distortions (along with asymmetric solvent–solute interactions when explicit waters are used) can promote this otherwise forbidden transition.

The bottom of Figure 7 is an attempt to isolate the effect that the geometry about the phenyl chromophore has on the molar rotation of phenylalanine. As with the carboxylate chromophore, the phenyl group has a local 2-fold axis of symmetry, which is why the left side of the bottom chart is identical to the right side, just as is the case in the top half of the figure. Also, when the $C_\alpha-C_\beta-C_\gamma-C_\delta$ dihedral angle passes through $\pm 90^\circ$, when the rest of the phenylalanine molecule is aligned perpendicular to the phenyl ring (in one of its mirror planes), then the molar rotation of the molecule is at a minimum. When this angle deviates from 90° , the molar rotation of the molecule deviates in a positive direction if the change in the dihedral is positive and in a negative direction if the dihedral change is negative. Logically, the opposite effect should be seen as the $C_\alpha-C_\beta-C_\gamma-C_\delta$ dihedral angle passes through 0° or 180° ; however, these are energetically disfavored angles, and the molecule is not found in configurations close to this angle often enough to make a determination on the chirality in the vicinity of these energetic maxima.

We expected this variation of optical rotation with the dihedral angle about the phenyl group to be consistent with the historical rationale for chiroptical response caused by the phenyl chromophore: as with the carboxylate chromophore, the space about the phenyl group can be divided into sectors, and the location of the atoms perturbing that space is connected with the sign of the response.^{52–54} However the “sectors” that our calculations allude to are of the opposite sign of those illustrated in Smith and co-worker’s illustrations of the sector rules in the works cited above. In 2002, with the aid of *ab initio* methods that the originators of these sector rules did not have the benefit of, Butz and co-workers obtained results similar to ours.⁵⁵ This led Butz et al. to set forth a revised sector rule for the benzene chromophore, which is quite similar to the historical model, except with the signs reversed.^{56,57} Our results here are consistent with this revised sector rule.

We have earlier demonstrated that an illustration of a sector rule for chiroptical response can be generated by a series of first-principles calculations on the chromophore of interest perturbed by a point charge in varying positions.⁴³ Here, we illustrate the molar rotation caused by a phenyl chromophore, approximated as a benzene molecule, as it is perturbed by a point charge of -0.1 , which has been shown to reasonably approximate the perturbing effects of the remainder of a zwitterionic amino acid molecule. The results are illustrated in Figure 8.

The sectors computed in Figure 8 all exhibit the D_{6h} symmetry of the benzene ring as they must, and as such give us sectors similar to those predicted by Schellman over four decades earlier.⁵⁸ One fact is consistent throughout the first three CD transitions shown, corresponding to the 1L_b , 1L_a , and half of the 1B_b excitations:⁵⁹ all have the same sign in the region outside of the hydrogen atoms on the benzene ring. As such, in this outer region, where the rest of a phenylalanine molecule is attached, the CD excitations reinforce to give the molar rotation shown on the left of Figure 8. Note these sectors fit with the revised sector rule of Butz et al.,⁵⁵ and are precisely the opposite of the historical sector rule cited by Pescitelli et al.⁶⁰

One aspect where our results are similar to those of Pescitelli and co-workers is in the basis set effects on the CD of aromatic compounds. We have found that the addition of diffuse functions to benzene and phenylalanine promotes excitations to diffuse electronic states, some of which occur at lower energies than the first three valence excitations expected from a simple LCAO model. This model has become the *de facto* standard model for benzene excitations used in textbooks. It has been used by Platt to assign the electronic spectrum of aromatic compounds and is the basis for the benzene sector rule.⁵⁹ To create the sector maps of Figure 8 we have used the SVP basis set which yields a collection of electronic excitations and energetic ordering consistent with the LCAO model. Similar results are obtained with the cc-pVDZ basis. Using a diffuse basis (aug-cc-pVDZ, d-aug-cc-pVDZ, etc., or a large set of diffuse s-, p-, d-functions added at the benzene ring center) yielded among the classic b1u, b2u, and e1u transitions several other electronic transitions of differing symmetries. The additional states were obtained both with TDDFT and with an approximate coupled cluster method (CC2). Since the energetic ordering depended on where the perturbing charge was

Table 1. Room Temperature Populations of the Conformers of Proline and Alanine in Solution^a

proline	C _γ endo	C _γ exo
molecular dynamics	66.0	34.0
Boltzmann, DFT optimized	65.5	34.5
experimentally derived	63	37

phenylalanine	h	g	t
molecular dynamics	29.4	34.3	36.3
Boltzmann, DFT optimized	21.5	3.1	75.5
experimentally derived	27	24	50

^a Experimental data are derived from nuclear magnetic resonance measurements and are from the works of Jankowski et al.⁶¹ and Fujiwara et al.⁶² for proline and phenylalanine, respectively. The DFT derived Boltzmann populations are from our previous work.⁴³

located this situation made it impossible to plot the CD sector maps for the b1u, b2u, and e1u transitions in an automated fashion using a diffuse basis. Fortunately, the sectors for molar rotation, which are affected to varying extents by all CD transitions, remain the same between different basis sets in the “substitution region” outside the carbon ring. While the basis set effects on the ordering of electronic excitations may warrant further investigation, they do not appear to affect conclusions regarding molar rotation aimed at in this work.

Comparison with Experiment

We shall finish this study with a discussion of how the modeling method being presented compares with those previously published, and with experimental data. Glycine is achiral, and its molar rotation should converge to zero over the course of the MD, as has been shown in our preliminary work. Proline and phenylalanine are both chiral molecules that adopt multiple conformations, all of which contribute to the average molar rotation that is observed experimentally. The modeling of the conformational distributions and the ultimate average molar rotations that result are discussed in turn.

The chiroptical properties measured in the laboratory are the result of the interaction of polarized light with molecules in varying conformations. Proline is known to be found in and around two local energetic minima, while phenylalanine has three local minima, illustrated earlier in Figures 6 and 7, respectively. In our earlier works the molecules were optimized to their respective structures, and the populations of the conformers determined by employing their computed relative energies using Boltzmann factors at room temperature. In this work, the “populations” were determined by a molecular dynamics simulation, and are classified on the basis of their dihedral angles. Proline molecules with a negative C_α–C_β–C_γ–C_δ dihedral angle were deemed to be of the C_γ endo conformation, and those with a positive angle were C_γ exo. For the phenylalanine molecule, the C_{acid}–C_α–C_β–C_γ dihedral is the determining factor, with h being –60° (±60), g being +60° (±60), and t being 180° (again ±60). These computed populations, along with experimentally derived data, are summarized in Table 1.

The agreement between dynamically computed populations, statically computed populations, and experimentally

Table 2. Average Molar Rotation of Proline and Phenylalanine^a

proline	C _γ endo	C _γ exo	average
molecular dynamics	–41.0	–68.1	–50.1
with TIP3P			
molecular dynamics	–53.9	–81.6	–63.3
with COSMO			
DFT optimized	–68.5	–125.5	–101.5
static with COSMO			
experiment			–99.2

phenylalanine	h	g	t	average
molecular dynamics	–96.2	–109.2	148.2	–11.9
with TIP3P				
molecular dynamics	–93.1	–125.5	149.4	–16.1
with COSMO				
DFT optimized	–128.1	124.7	–1.9	–36.8
static with COSMO				
experiment				–57.0

^a DFT optimized static data are from our previous work.⁴³ Experimental data are from Greenstein and Winitz.⁶³

derived populations for the proline conformers is excellent. As molar rotation depends in part upon these populations, it is apparent that the conformer distribution should not be a significant source of error for this molecule. In our previous work using static geometries, we found very good agreement between the modeled and measured chiroptical properties of proline.⁴¹ Because the populations of the conformers found by the dynamics simulations in this current work are the same, we thus expect any deviations in the fit of this dynamic model to be caused either by the geometric distortions (vibrations) of the molecular dynamics used to generate the structure, and by the use of a point charge solvation method instead of a continuum.

The agreement in conformer populations for phenylalanine is not as perfect as it is for proline. One aspect on which dynamic calculations, static calculations, and experimental derivations agree is that the phenylalanine rotamer in which the phenyl ring and carboxylate group are *trans* to each other is the most highly populated. What they do not agree upon is the extent of the dominance of this conformation: our previous work⁴² indicated that 3/4 of the molecules should be of this conformation, Fujiwara’s experimental data said this population should be closer to 1/2, and the current molecular dynamics puts it at just over 1/3 of the population. The dynamics data indicate a much more even distribution among the conformers than the earlier static computations, which is in somewhat better agreement with experiment. Therefore, we would expect a somewhat better agreement with experiment for the molar rotations modeled in this current work than in previous works. This comparison between the molar rotation from theory and experiment is shown in Table 2.

The molar rotation of proline computed with two optimized geometries and weighted by their Boltzmann factors is in excellent agreement with experiment, differing by only about 2 deg·cm²/(dmol). When thermal effects are added, by using structures taken from snapshots of the molecular dynamics simulation, this deviation increases to about 36 deg·cm²/(dmol). When TIP3P waters are substituted for the COSMO continuum, this deviation increases by another 13

$\text{deg}\cdot\text{cm}^2/(\text{dmol})$. While it is tempting to conclude that the agreement between theory and experiment is clearly worse with the dynamics model and explicit solvation, this is not so clearly the case because of other approximations, most notably those inherent in TDDFT. That is, the supposedly improved solvation treatment may well expose systematic errors in the TDDFT optical rotation computations. The results for phenylalanine are similar. Given the confidence level of time dependent density functional theory, the good agreement between theory and experiment using the static model might be fortuitous, and the data using the dynamics model may be equally as useful. As the field of first principles modeling of optical activity continues to develop, more advanced (and more costly) linear response electronic structure methods such as coupled cluster analyses may become more widely available in computing codes, and more powerful computers should make them practical, but for now TDDFT remains the state of the art method for modeling the optical activity of molecules of this size (and using as many MD configurations as done here).

Conclusions

Molecular dynamics and explicit solvation may be used to generate geometric data suitable for the modeling of molar rotation of conformationally flexible molecules by time dependent density functional theory. The molar rotations of the various conformers of the amino acids studied can be rationalized in terms of the sector rules for the carboxylate and phenyl chromophores. The inclusion of vibrational effects and explicit solvent effects via molecular dynamics both dampened the magnitude of the average molar rotations computed for the molecules studies. The damping effect can also be traced back to the sector rules, this time via a lack of presence of a perturbing group in a given sector. The results highlight the difficulties of obtaining reliable optical rotations for conformationally flexible molecules.

References

- (1) Crawford, T. D.; Stephens, P. J. *J. Phys. Chem. A* **2008**, *112*, 1339.
- (2) Grimme, S.; Muck-Lichtenfeld, C. *Chirality* **2008**, *20*, 1009.
- (3) Pecul, M.; Ruud, K. The ab initio calculation of optical rotation and electronic circular dichroism. In *Advances In Quantum Chemistry*; Elsevier Academic Press Inc: San Diego, 2005; Vol. 50, p 185.
- (4) Stephens, P. J.; McCann, D. M.; Cheeseman, J. R.; Frisch, M. J. *Chirality* **2005**, *17*, S52.
- (5) Giorgio, E.; Tanaka, K.; Verotta, L.; Nakanishi, K.; Berova, N.; Rosini, C. *Chirality* **2007**, *19*, 434.
- (6) Jansik, B.; Rizzo, A.; Agren, H. *J. Phys. Chem. B* **2007**, *111*, 446.
- (7) Tanaka, T.; Kodama, T. S.; Morita, H. E.; Ohno, T. *Chirality* **2006**, *18*, 652.
- (8) Kongsted, J.; Pedersen, T. B.; Jensen, L.; Hansen, A. E.; Mikkelsen, K. V. *J. Am. Chem. Soc.* **2006**, *128*, 976.
- (9) Autschbach, J. *Comput. Lett.* **2007**, *3*, 131.
- (10) Crawford, T. D.; Tam, M. C.; Abrams, M. L. *J. Phys. Chem. A* **2007**, *111*, 12057.
- (11) Wiberg, K. B.; Wang, Y. G.; Wilson, S. M.; Vaccaro, P. H.; Jorgensen, W. L.; Crawford, T. D.; Abrams, M. L.; Cheeseman, J. R.; Luderer, M. *J. Phys. Chem. A* **2008**, *112*, 2415.
- (12) Kapitan, J.; Baumruk, V.; Kopecky, V.; Bour, P. *J. Phys. Chem. A* **2006**, *110*, 4689.
- (13) Tam, M. C.; Crawford, T. D. *J. Phys. Chem. A* **2006**, *110*, 2290.
- (14) Carlson, K. L.; Lowe, S. L.; Hoffmann, M. R.; Thomasson, K. A. *J. Phys. Chem. A* **2006**, *110*, 1925.
- (15) Mori, T.; Inoue, Y.; Grimme, S. *J. Org. Chem.* **2006**, *71*, 9797.
- (16) Marchesan, D.; Coriani, S.; Forzato, C.; Nitti, P.; Pitacco, G.; Ruud, K. *J. Phys. Chem. A* **2005**, *109*, 1449.
- (17) da Silva, C. O.; Mennucci, B.; Vreven, T. *J. Org. Chem.* **2004**, *69*, 8161.
- (18) Voloshina, E.; Raabe, G.; Estermeier, M.; Steffan, B.; Fleischhauer, J. *Int. J. Quantum Chem.* **2004**, *100*, 1104.
- (19) Kondru, R. K.; Wipf, P.; Beratan, D. N. *J. Phys. Chem. A* **1999**, *103*, 6603.
- (20) Kundrat, M. D.; Autschbach, J. *J. Chem. Theory Comput.* **2008**, *4*, 1902.
- (21) Mort, B. C.; Autschbach, J. *J. Phys. Chem. A* **2005**, *109*, 8617.
- (22) Mort, B. C.; Autschbach, J. *J. Phys. Chem. A* **2006**, *110*, 11381.
- (23) Mort, B. C.; Autschbach, J. *ChemPhysChem* **2007**, *8*, 605.
- (24) Mort, B. C.; Autschbach, J. *ChemPhysChem* **2008**, *9*, 159.
- (25) Wilson, S. M.; Wiberg, K. B.; Murphy, M. J.; Vaccaro, P. H. *Chirality* **2008**, *20*, 357.
- (26) Crawford, T. D.; Tam, M. C.; Abrams, M. L. *Mol. Phys.* **2007**, *105*, 2607.
- (27) Kongsted, J.; Pedersen, T. B.; Strange, M.; Osted, A.; Hansen, A. E.; Mikkelsen, K. V.; Pawlowski, F.; Jorgensen, P.; Hattig, C. *Chem. Phys. Lett.* **2005**, *401*, 385.
- (28) Pecul, M.; Marchesan, D.; Ruud, K.; Coriani, S. *J. Chem. Phys.* **2005**, 122.
- (29) Kongsted, J.; Pedersen, T. B.; Osted, A.; Hansen, A. E.; Mikkelsen, K. V.; Christiansen, O. *J. Phys. Chem. A* **2004**, *108*, 3632.
- (30) Kongsted, J.; Ruud, K. *Chem. Phys. Lett.* **2008**, *451*, 226.
- (31) Neugebauer, J. *Angew. Chem., Int. Ed.* **2007**, *46*, 7738.
- (32) Mukhopadhyay, P.; Zuber, G.; Wipf, P.; Beratan, D. N. *Angew. Chem., Int. Ed.* **2007**, *46*, 6450.
- (33) Mukhopadhyay, P.; Zuber, G.; Goldsmith, M. R.; Wipf, P.; Beratan, D. N. *ChemPhysChem* **2006**, *7*, 2483.
- (34) Jensen, L.; Swart, M.; Van Duijnen, P. T.; Autschbach, J. *Int. J. Quantum Chem.* **2006**, *106*, 2479.
- (35) Wilson, S. M.; Wiberg, K. B.; Cheeseman, J. R.; Frisch, M. J.; Vaccaro, P. H. *J. Phys. Chem. A* **2005**, *109*, 11752.
- (36) Mennucci, B.; Tomasi, J.; Cammi, R.; Cheeseman, J. R.; Frisch, M. J.; Devlin, F. J.; Gabriel, S.; Stephens, P. J. *J. Phys. Chem. A* **2002**, *106*, 6102.
- (37) Coriani, S.; Baranowska, A.; Ferrighi, L.; Forzato, C.; Marchesan, D.; Nitti, P.; Pitacco, G.; Rizzo, A.; Ruud, K. *Chirality* **2006**, *18*, 357.

- (38) Pecul, M.; Larnparska, E.; Cappelli, C.; Frediani, L.; Ruud, K. *J. Phys. Chem. A* **2006**, *110*, 2807.
- (39) Rossi, S.; Lo Nostro, P.; Lagi, M.; Ninham, B. W.; Baglioni, P. *J. Phys. Chem. B* **2007**, *111*, 10510.
- (40) Lo Nostro, P.; Ninham, B. W.; Milani, S.; Fratoni, L.; Baglioni, P. *Biopolymers* **2006**, *81*, 136.
- (41) Kundrat, M. D.; Autschbach, J. *J. Phys. Chem. A* **2006**, *110*, 4115.
- (42) Kundrat, M. D.; Autschbach, J. *J. Phys. Chem. A* **2006**, *110*, 12908.
- (43) Kundrat, M. D.; Autschbach, J. *J. Am. Chem. Soc.* **2008**, *130*, 4404.
- (44) Ahlrichs, R.; Bar, M.; Haser, M.; Horn, H.; Kolmel, C. *Chem. Phys. Lett.* **1989**, *162*, 165.
- (45) Woon, D. E.; Dunning, T. H. *J. Chem. Phys.* **1994**, *100*, 2975.
- (46) Schafer, A.; Klamt, A.; Sattel, D.; Lohrenz, J. C. W.; Eckert, F. *Phys. Chem. Chem. Phys.* **2000**, *2*, 2187.
- (47) Lindahl, E.; Hess, B.; van der Spoel, D. *J. Mol. Model.* **2001**, *7*, 306.
- (48) Jorgensen, W. L.; Maxwell, D. S.; TiradoRives, J. *J. Am. Chem. Soc.* **1996**, *118*, 11225.
- (49) Wiberg, K. B.; Wang, Y. G.; Vaccaro, P. H.; Cheeseman, J. R.; Luderer, M. R. *J. Phys. Chem. A* **2005**, *109*, 3405.
- (50) Pecul, M.; Ruud, K.; Rizzo, A.; Helgaker, T. *J. Phys. Chem. A* **2004**, *108*, 4269.
- (51) Jorgensen, E. C. *Tetrahedron Lett.* **1971**, *13*, 863.
- (52) Smith, H. E.; Fontana, L. P. *J. Org. Chem.* **1991**, *56*, 432.
- (53) Smith, H. E.; Neergaard, J. R. *J. Am. Chem. Soc.* **1997**, *119*, 116.
- (54) Smith, H. E. *Chem. Rev.* **1998**, *98*, 1709.
- (55) Butz, P.; Tranter, G. E.; Simons, J. P. *PhysChemComm* **2002**, 91.
- (56) Macleod, N. A.; Butz, P.; Simons, J. P.; Grant, G. H.; Baker, C. M.; Tranter, G. E. *Isr. J. Chem* **2004**, *44*, 27.
- (57) Macleod, N. A.; Butz, P.; Simons, J. P.; Grant, G. H.; Baker, C. M.; Tranter, G. E. *Phys. Chem. Chem. Phys.* **2005**, *7*, 1432.
- (58) Schellman, J. A. *J. Chem. Phys.* **1966**, *44*, 55.
- (59) Platt, J. R. *J. Chem. Phys.* **1949**, *17*, 484.
- (60) Pescitelli, G.; Di Bari, L.; Caporusso, A. M.; Salvadori, P. *Chirality* **2008**, *20*, 393.
- (61) Jankowski, K.; Soler, F.; Ellenberger, M. *J. Mol. Struct.* **1978**, *48*, 63.
- (62) Fujiwara, S.; Ishizuka, H.; Fudano, S. *Chem. Lett.* **1974**, *11*, 1281.
- (63) Greenstein, J. P.; Winitz, M. *Chemistry of the Amino Acids*; John Wiley & Sons: New York, 1961.

CT8005216